J Mater Sci (2007) 42:6929–6934
DOI 10.1007/s10853-006-1330-y

Disordering and the electronic transport behaviors of NbC–Al_4C_3–C composite

D. Li · S. Ma · W. F. Li · B. Wu · Z. D. Zhang

Received: 17 August 2006 / Accepted: 28 November 2006 / Published online: 26 April 2007

Abstract A composite nanomaterial composed of NbC nanocrystals, Al_4C_3 nanorods and carbon nanofibers as well as amorphous carbon was fabricated by arc-discharging a Nb_3Al block as an anode in CH_4 gas. The growth process of the NbC–Al_4C_3–C composite was deduced according to the microstructures of its components and the experimental conditions. NbC nanocrystals with non-stoichiometric chemical composition were in a cubic shape. As the decomposition product of the precursor of CH_4 gas, carbon nanofibers were thought to be as templates, reacting with Al atoms, to form Al_4C_3 nanorods with a diameter of 15–40 nm. A thin layer of aluminum carbide oxide covered the surface of Al_4C_3 nanorods. The temperature dependence of the resistivity for the NbC–Al_4C_3–C composite was described by the variable-range-hopping (VRH) model between about 100 K and 300 K because of the strong localization of electrons by disorder in the carbon matrix. Below 100 K, the transport behaviors of the pellet deviated from the VRH model due to the conduction competition between the semi-conducting carbon matrix and metallic NbC nanocrystals.

Introduction

The discovery of carbon nanotubes [1] has aroused a great deal of interest for physicists investigating one-dimensional (1D) nanostructured systems [2, 3]. Because of the novel physics behaviors, the 1D nanomaterials possess a wide range of potential applications in future on mesoscopic electronic and optoelectronic devices [4, 5]. Carbon nanotubes have been used as templates to fabricate other 1D nanomaterials [6–10]. Recently, the Al_4C_3 nanowires and nanoribbons were synthesized in a solid-state reaction using lithium as a catalyst [11]. When we aimed to study the superconductivity of NbC nanoparticles, a composite material consisted of NbC(C) nanocapsules and carbon nanofibers was synthesized by arc discharging a Nb block in CH_4 [12]. Here we reported a composite nanomaterial including carbon nanofibers, Al_4C_3 nanorods and NbC nanoparticles produced by arc discharging a Nb_3Al block in CH_4, where carbon nanofibers were thought as templates to fabricate the Al_4C_3 nanorods. The microstructures of the composite components were characterized by transmission electron microscopy and their growth processes were deduced. Disordering and the electronic transport behaviors of NbC–Al_4C_3–C nanocomposites were studied and discussed in details.

Experimental details

The NbC–Al_4C_3–C composites were prepared by the arc discharge process, developed in the previous work [12–14]. Argon (20,000 Pa) was introduced into an evacuated chamber (7×10^{-3} Pa). An arc between carbon rod in a diameter of 3 mm and a Nb_3Al block started to be stable with a current of 100 A. Then, CH_4 gas (4,000 Pa) was rapidly introduced into the chamber. The mixed gas was served as reactant gas and a source of hydrogen plasma. When the current was maintained at 100 A and a potential sustaining in a range of 22–24 V between the cathode and

D. Li (✉) · S. Ma · W. F. Li · B. Wu · Z. D. Zhang
Shenyang National Laboratory for Materials Science, Institute of Metal Research and International Center for Materials Physics, Chinese Academy of Sciences, 72 Wenhua Road, Shenyang 110016, P.R. China
e-mail: dali@imr.ac.cn

the anode during the whole preparation, bulk Nb_3Al was evaporated while CH_4 decomposed into C and [H]. Consequently, NbC–Al_4C_3–C composites were condensed on the internal surface of the work chamber. Once the arc discharge process was finished, residual gases were pumped out and Ar gas with a pressure 50,000 Pa was introduced for the products passivation. Deposits on the water-cooled wall of the chamber were collected and stored in air.

X-ray diffraction (XRD) patterns were recorded at room temperature on a D/max-γA diffractometer with Cu K_α radiation under 50 kV and 250 mA. The morphology and structure of the as-prepared powders were observed by JEOL 2010 EX transmission electron microscopy (TEM), while the chemical composition was analyzed by means of energy dispersive X-ray (EDX) spectroscopy. Structural disorder of carbon in the as-prepared NbC–Al_4C_3–C composites was estimated by Raman spectrum. For resistivity measurements, the NbC–Al_4C_3–C composite was pressed into a pellet in a diameter of 10 mm by using a 1.2 GPa axial pressure with a steel die. DC magnetic susceptibility and electrical resistivity of the NbC–Al_4C_3–C composite were measured by using a superconducting quantum interference device (SQUID, Quantum design) magnetometer.

Results and discussion

Figure 1 shows the XRD pattern of the NbC–Al_4C_3–C composite. The diffraction peaks could be indexed as cubic NbC, C, Al_4C_3 (ICDD card no. 35-799), δ-Al_4C_3 (ICDD card no. 35-799), and Al_2OC. XRD peaks, corresponding to carbon, shift to lower angles, which indicate a lattice expansion. The temperature dependences of the dc magnetic susceptibility of the composite measured in a magnetic field of 50 Oe did not show the superconducting transition of NbC nanocrystals. It is very different from our previous NbC nanocrystal prepared by arc discharging a pure Nb anode in CH_4 [12]. Niobium carbide (NbC_x) generally exhibits a wide range of non-stoichiometry that x values can shift from 0.75 to 1 with attendant carbon vacancy sites, causing the significant change of its physical and chemical properties. The high electrical conductivity and superconductivity have been only observed in the stoichiometric NbC specimens [15]. It means that the chemical composition of NbC nanocrystals, obtained by the arc discharging using a bulk Nb_3Al as the anode, is non-stoichiometric. According to the XRD data of the NbC nanocrystals, the lattice constant of NbC nanocrystals was a = 4.465 Å. It was reported that there was the following relationship between lattice parameter a and carbon content x in NbC_x [16]: a (Å) = 4.09847 + 0.71820x–0.34570x^2. By using this relationship, the x value is calculated to be 0.90. The NbC nanocrystals are non-stoichiometric, thus no superconducting transition occurs.

A TEM micrograph (Fig. 2) exhibits that the NbC–Al_4C_3–C composite prepared in a CH_4 atmosphere consists of nanorods, nanoparticles, and nanofibers. The corresponding EDX analysis (as shown in Fig. 3a and b) of the NbC–Al_4C_3–C composite indicates that the nanofibers are mainly composed of carbon, while the nanorods contain the elements of Al, C and O, respectively. Copper detected in Fig. 3 comes from the copper grid, which is coated with thin carbon film used to mount the powder specimens. Figure 4a presents the microstructure of the nanofiber component in the composite material. High Resolution

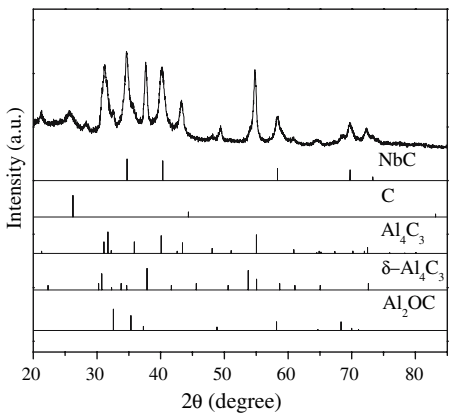

Fig. 1 XRD patterns of the NbC–Al_4C_3–C composite with the existence of NbC, C, Al_4C_3, δ-Al_4C_3, and Al_2OC phases. For comparison, the corresponding theoretical XRD patterns for the different phases are represented below the experimental data

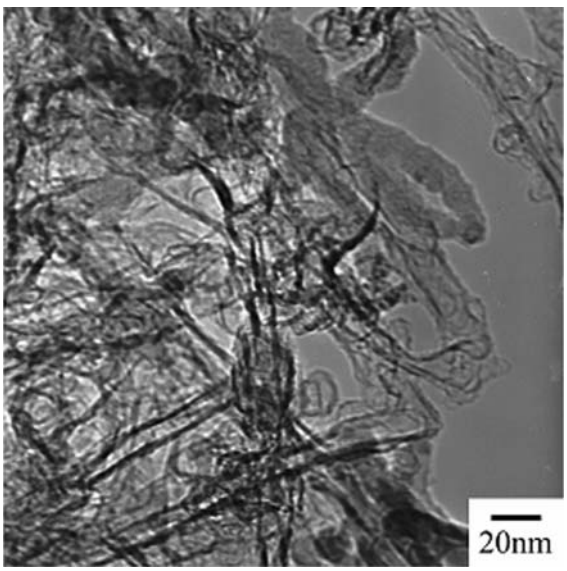

Fig. 2 TEM bright field image of the NbC–Al_4C_3–C composite nanomaterial

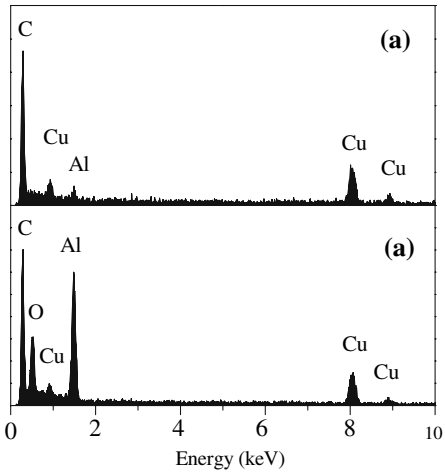

Fig. 3 Energy dispersive X-ray analysis (EDX) patterns for (**a**) carbon nanofibers and (**b**) Al_4C_3 nanorods

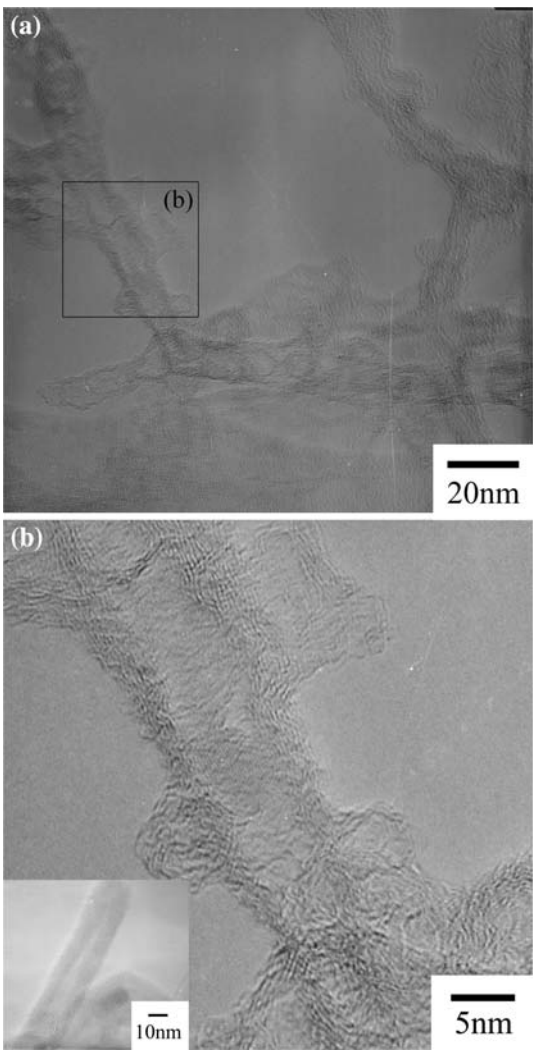

Fig. 4 (**a**) HRTEM bright field image of C nanofibers and (**b**) the enlarged part of the C nanofiber like a hollow tree trunk. The inset of (**b**) shows a different microstructure of C nanotube

Transmission Electron Microscopy (HRTEM) image (Fig. 4b) indicates a very complex hollow-trunk like microstructure. The carbon nanofibers are in crystal form with amorphous edges. As well, a small amount of carbon nanotubes in crystal form can be found as shown in the inset of Fig. 4b.

A typical morphology of the Al_4C_3 nanorods (diameters from 15 to 40 nm) is shown in Fig. 5a. The corresponding diffraction pattern presented as the inset of Fig. 5a revealed that the Al_4C_3 nanorod grew along the [001] direction, in good agreement with the growth of Al_4C_3 nanowires synthesized by solid-state reaction [11]. Detailed investigation on Al_4C_3 nanorod in Fig. 5b shows a thin layer on its surface, which is determined to be aluminum carbide oxide according to the analysis of EDX results. Because there are excess carbon atoms during the formation of the Al_4C_3 nanorods, it is possible that aluminum carbide oxide (but not aluminum oxide) could be fabricated in our system. It is different from the previous report [11] that the surface of Al_4C_3 nanowires and nanobelts were coated by aluminum oxide. Figure 6 shows that NbC nanocrystals are dispersed in the composite. The amount of NbC nanocrystals is much less than that of carbon nanofibers and Al_4C_3 nanorods and the particle size (about 2–12 nm) of the former is also very small. Figure 6b exhibits a higher magnification of TEM image of NbC nanocrystals, which clearly shows no shell coating on the surface of the NbC nanocrystals. It very differs from the core/shell structure of NbC(C) nanocapsules prepared by arc discharging a Nb block in CH_4 [12].

The growth process for the composite NbC–Al_4C_3–C nanomaterial is very complicated. As soon as the Nb_3Al anode is ionized by arc-discharge, the Nb and Al atoms are released. At the same time, C atoms are produced by the decomposition of CH_4 and the evaporation of C cathode. The composition of the vapor can be attributed to different evaporating pressures of the elements during the arc-discharging process. For an evaporating pressure of 133 Pa (1 torr), the corresponding temperatures are 1,560 °C (Al), 2,897 °C (C), and 3,177 °C (Nb), respectively [17]. From the experimental results [18], it is clear that the higher the evaporating pressure of the element, the higher its amount in the nanocapsules. It is the reason that the NbC–Al_4C_3–C composite consists of main Al_4C_3 and C with a small amount of NbC nanocrystals. Besides the evaporating pressures, the melting points of the carbides (NbC 3,610 °C, Al_3C_4 2,100 °C), carbon (3,527 °C) and Al (660.4 °C) are important factors in the growth process for the composite. The formation of the products also depended on the kinetic process. The velocities distribution of different atoms in a non-equilibrium process can be related to the molecular mass and the temperature by the Boltzmann function. Comparing the metal molecular velocities of Al and Nb, one finds that Al is about a

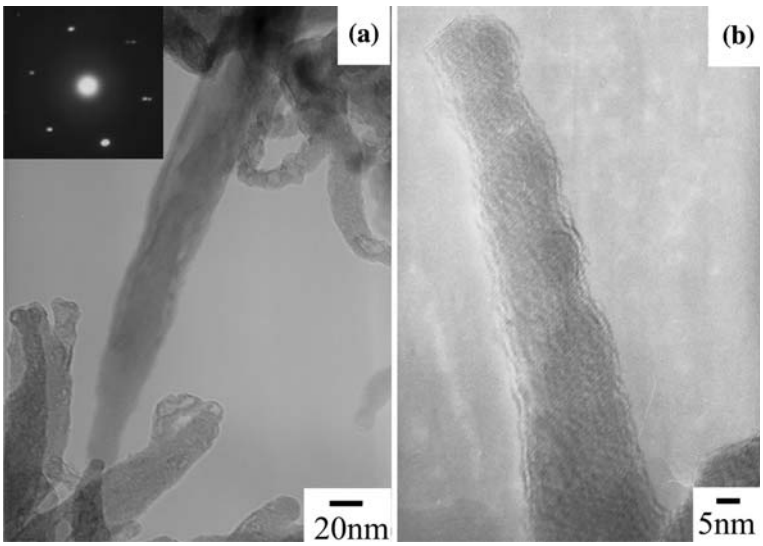

Fig. 5 (**a**) TEM bright field image and the corresponding selected area electron diffraction (SAED) pattern of Al_4C_3 nanorods in the NbC–Al_4C_3–C composite and (**b**) HRTEM image of an Al_4C_3 nanorod

few times faster than Nb because of the different masses. As the temperature is gradually lowered, the Nb atoms will combine with C atoms to form NbC nanocrystals and the excess C atoms grow into carbon nanofibers as well as amorphous carbon. Then, a large amount of Al atoms in the present vapor can preferentially react with carbon to form Al_4C_3. The boiling point of Al_4C_3 is about 2,200 °C, above which Al_4C_3 will decompose. Similar to our previous work [12], NbC(C) nanocapsules with a core/shell structure would be obtained. However, as shown in Fig. 6b, the cubic NbC nanocrystals collected in the present composite are coated by nothing. It is thought that the thin carbon layers on the surface of the NbC(C) nanocapsules reacted with Al atoms to form gaseous Al_4C_3 at its boiling temperature of 2,200 °C. In the carbides of niobium, only carbon atoms diffuse to some extent, while the niobium sublattice is fixed [19]. As the carbon shell on the NbC nanocrystal was used up, the inter-diffusion of carbon atoms from the inside of NbC nanocrystal to its surface would happen. Therefore, NbC nanocrystals could loss a small amount of carbon, which may result in the non-stoichiometric NbC nanocrystals without superconductivity. As the temperature decreases, the Al_4C_3 vapor would condense to form Al_4C_3 nanoparticles. That NbC nanocrystals were not coated by aluminum carbide may be caused by their bad wetting ability. Below 2,200 °C, the Al vapor would be also adsorbed on the surface of carbon nanofibers to lower the total free energy. Aluminum and graphite were known to react to form Al_4C_3 above 1,000 °C [20]. The 1D Al_4C_3 nanorods were fabricated when carbon nanofibers were used as templates for the reaction of Al and C atoms. It indicates that the synthesis of the 1D Al_4C_3 nanorods was carried out using a precursor of CH_4 gas, which is very different from the previous works [6–10] using carbon nanotubes as precursors to prepare other 1D nanomaterials.

The Raman spectrum of the present composite material exhibits a graphite G band at 1,593 cm^{-1}, E_{2g} mode corresponding to in-plane vibration of aromatic carbons, and a D band at 1,335 cm^{-1}, indicating the structural disorder feature of carbon (sp^2). The highly structural disorder of the carbon components in our composite can cause a strong localization of transport electrons and the conductivity of the material can be described by hopping conduction. In a three-dimensional case, the temperature dependence of the hopping conductivity is derived by Mott [21] as:

$$\sigma(T) = \sigma_0 \exp\left(-\frac{T_0}{T}\right)^{1/4}$$

where σ_0 is a material constant and T_0 corresponds to a characteristic temperature of the system. As represented in Fig. 7, a good linear fit between a temperature range of about 100 K and 300 K is satisfactory with the experimental data of the pellets. It indicates that the conductivity of the specimen pellets in this temperature range is dominated by the carbon matrix, in terms of the variable-range-hopping (VRH) model. As decreasing the temperature below 100 K, the fitting lines deviated from the resistivity $\ln\rho$ (T) curves because the metallic NbC nanocrystals would involve in the electronic transport of the pellets. The resistivity of the metallic NbC nanocrystals decreases with decreasing the temperature, while that of the carbon matrix increases. As a result, the deviation of the fitting lines from the experimental data should be caused by the conduction competition of the semi-conducting carbon and metallic NbC nanocrystals.

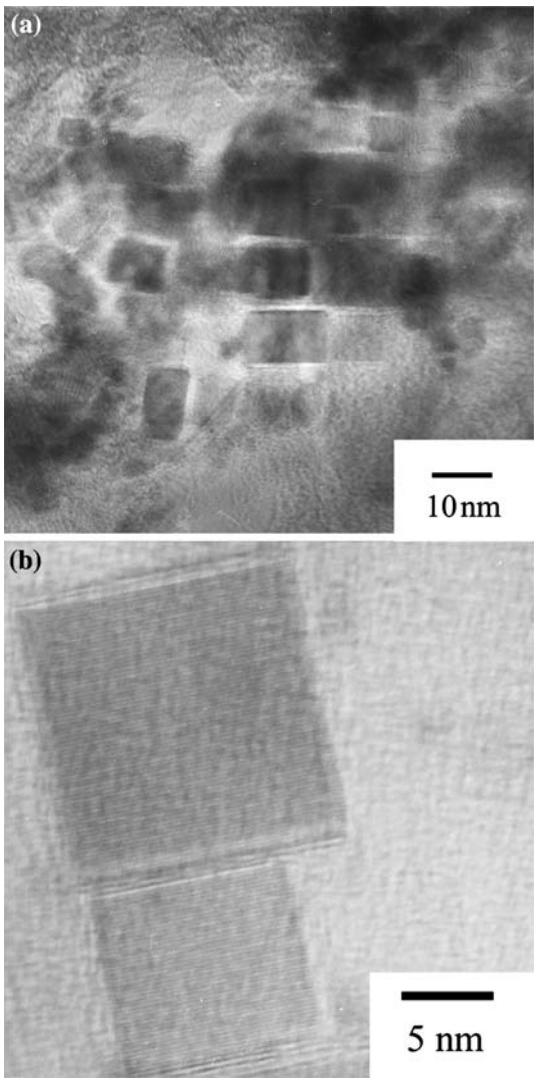

Fig. 6 (**a**) TEM bright field image of the cubic NbC nanocrystals in the NbC–Al_4C_3–C composite and (**b**) HRTEM image of NbC nanocrystals

Conclusions

A composite nanomaterial of NbC–Al_4C_3–C was fabricated by arc-discharging Nb_3Al block as the anode in a methane (CH_4) atmosphere. Magnetic and electrical measurements indicate that the cubic NbC nanocrystals are not superconducting because of their non-stoichiometric chemical composition. The 1D Al_4C_3 nanorods were formed on the templates of carbon nanofibers. The surface of Al_4C_3 nanorod was covered by a thin layer of aluminum carbide oxide. As well, a large amount of carbon nanofibers and amorphous carbon were obtained. The carbon nanofibers with complex microstructures were consisted of both crystalline and amorphous components. Carbon components in the composite exhibited a high degree of disorder as characterized by a D band in the Raman spectrum. The

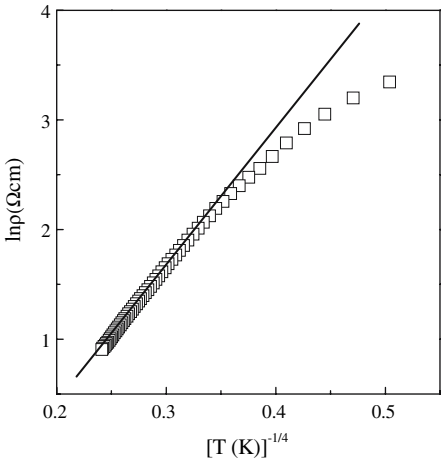

Fig. 7 Plots of the resistivity ρ on a logarithmic scale against $T^{-1/4}$ for the as-prepared NbC–Al_4C_3–C pellet. The open square is for the experimental data, while the line shows the linearity of the plot

temperature dependence of the electrical resistivity of the pellet was attributed to the VRH model in between about 100 K and 300 K due to the strong localization of electrons by the disorder of carbon matrix. Below 100 K, the electronic transport behavior of the pellet did not follow the VRH conduction because of the competition of the semiconducting carbon matrix and the metallic NbC nanocrystals.

Acknowledgments The work has been supported by National Natural Science Foundation of China under grant numbers No. 50332020 and No. 50171070.

References

1. Iijima S (1991) Nature 354:56
2. Ebbesen TW, Ajayan PM (1992) Nature 358:220
3. Huang MH, Mao S, Feick H, Yan HQ, Wu YY, Kind H, Weber E, Russo R, Yang PD (2001) Science 292:1897
4. Hu J, Odom TW, Lieber CM (1999) Acc Chem Res 32:435
5. Dekker C (1999) Phys Today 52:22
6. Fukunaga A, Chu S, McHenry ME (1999) J Mater Sci Lett 18:431
7. Fukunaga A, Chu SY, McHenry ME (1998) J Mater Res 13:2465
8. Shi L, Gu YL, Chen LY, Yang ZH, Ma JH, Qian YT (2005) Carbon 43:211
9. Wu HQ, Wei XW, Shao MW, Gu JS (2004) J Cryst Growth 265:184
10. Wu HQ, Wei XW, Shao MW, Gu JS (2002) Chem Phys Lett 364:152
11. Zhang HF, Dohnalkova AC, Wang CM, Young JS, Buck EC, Wang LS (2002) Nano Lett 2:105
12. Li D, Li WF, Ma S, Zhang ZD (2006) Phys Rev B 73:193402
13. Dong XL, Zhang ZD, Chuang YC, Jin SR (1999) Phys Rev B 60:3017
14. Zhang ZD, Yu JL, Zheng JG, Skorvanek I, Kovac J, Dong XL, Li ZJ, Jin SR, Yang HC, Guo ZJ, Liu W, Zhao XG (2001) Phys Rev B 64:024404

15. Pechen EV, Krasnosvobodtsev SI, Shabanova NP, Ekimov EV, Varlashkin AV, Nozdrin VS, Tschovrebov AM, Golovashkin AI (1994) Physics C 235–240:2511
16. Storms EK (1967) The refractory carbides. Academic Press, New York, NY, p 65
17. Zhang ZX (1979) Handbook of physical constants. Beijing, Science Press, p 84 (in Chinese)
18. Geng DY, Zhang ZD, Zhang WS, Si PZ, Zhao XG, Liu W, Hu KY, Jin ZX, Song XP (2003) Scr Mater 48:593
19. Woodford J, Chang YA (1998) Metall Mater Trans A 29:2717
20. Cotton FA, Wilkinson G (1988) Advanced inorganic chemistry, 5th edn. Wiley, New York
21. Mott NF (1970) Phil Mag 22:7